To cite this article: CHU R T, LIU Z Q. Ship course sliding mode control system based on FTESO and sideslip angle compensation [J/OL]. Chinese Journal of Ship Research, 2022, 17(1). http://www.ship-research.com/en/article/doi/10.19693/j.issn.1673-3185.02267.

DOI: 10.19693/j.issn.1673-3185. 02267

Ship course sliding mode control system based on FTESO and sideslip angle compensation

CHU Ruiting, *LIU Zhiquan**

Key Laboratory of Transport Industry of Marine Technology and Control Engineering, Ministry of Transport, Shanghai Maritime University, Shanghai 201306, China

Abstract: [**Objectives**] To improve the course tracking performance and reduce the course error of an underactuated surface ship, this paper studies a ship course sliding mode control system based on the finite-time extended state observer (FTESO). [**Methods**] A prefilter is adopted to reduce the influence of the high course change rate during the steering. The time-varying sideslip angle is estimated by FTESO, and the course error is corrected by the estimated sideslip angle in a timely manner. To simplify the design of the controller, the external disturbance and internal uncertainty in the yaw direction are estimated by the observer simultaneously and compensated in the controller design. Considering the input saturation constraint, this paper selects a sliding mode surface with an integral term and designs the sliding mode control law by FTESO, and it finally proves the stability of the control system by the Lyapunov stability theory. [**Results**] The simulation results show that the proposed control system reduces the course tracking error and makes it converge to zero in a shorter time. [**Conclusions**] The results of this study can provide references for the course tracking control design of surface ships.

Key words: ship course control; sideslip angle; sliding mode control; finite-time extended state observer (FTESO); input saturation constraint

CLC number: U664.82

0 Introduction

With the development of the global marine industry, ship motion control has attracted more attention, and course tracking is an important performance that cannot be ignored from beginning to end. In addition to the impact of sea-surface disturbance, the complexity and uncertainty of ship maneuvering also pose great challenges for the ship course control. Therefore, the discussion on the robust control algorithms is of practical significance to ship course control. At present, multiple control methods, e.g., state feedback linearization [1], backstepping[2], sliding mode control (SMC) [3] and adaptive control [4], fuzzy algorithm [5], and model predictive control (MPC) algorithm [6], have been extensively used in the field of ship control. In order to solve the practical application problems of high output energy and intractable nonlinear functions in the backstepping method, Zhang et al. [2] modulated the control error by using the sine function and improved the control performance of the ship autopilot without changing the controller structure. However, the control design of the nonlinear steering system of ships is generally affected by nonlinear impacts of rudder angle, rudder rate, and course angle. In order to simplify the nonlinear steering system of ships, Perera et al. [7] studied the input-out-

Received: 2021－01－16 **Accepted**: 2021－04－09

Supported by: National Natural Science Foundation of China (No. 52001197); Key Project of Capacity Building of Shanghai Local Colleges and Universities (No. 19040501600)

Authors: CHU Ruiting, female, born in 1997, master degree candidate. Research interest: ship course control. E-mail: 1398555801@qq.com

LIU Zhiquan, male, born in 1986, Ph.D., associate professor. Research interest: ship motion control. E-mail: liuzhiquan215@sina.com

***Corresponding author**: LIU Zhiquan

put linearization control methods based on Lyapunov, Hurwitz, and PID, but they have not yet solved the problem of complex sideslip angle in the path tracking control of underactuated surface ships [8].

For the sideslip angle compensation, the most direct way is to use GPS, accelerometer, and other sensors for measurement [9]; however, the noise and high cost of sensors make this method infeasible. Therefore, Wang et al. [10] proposed a line-of-sight (LOS) guidance law based on extended state observer (ESO) of filter, and the law uses FTESO to estimate the time-varying sideslip angles caused by current, wind, and wave disturbances, thereby achieving path tacking; however, they failed to consider the rudder saturation. Li et al. [11] designed a novel ESO which achieves effective ship course tracking by SMC. Compared with the conventional linear ESO (LESO), the nonlinear terms of FTESO can guarantee a finite-time estimation of an extended state. In order to improve the observational performance, Xiong et al. [12] proposed a novel ESO that reflects the output estimation error by nonlinear terms and switching terms; on the basis of the structure of the ESO, the problem affecting the design of the observer is transformed into a design problem of the state observer under external disturbances. Due to the mechanical characteristics, rudder saturation does exist in ship control; therefore, many researchers have conducted extensive studies on the analysis and the design methods of control systems with rudder saturation. Liang et al. [13] used FTESO to estimate the unmeasurable state of the dynamic positioning ship within finite time and constructed an auxiliary system to handle and control the saturation state. In addition, the control signal before entering the observer can also be limited by saturation function, so as to reduce the effect of actuator saturation constraint [14].

For the nonlinear characteristics and external disturbances in the ship course control, FTESO is used to estimate the unmeasurable state, and thus the sideslip angle estimation is obtained on the basis of time-varying sideslip angle and input saturation, thereby correcting the course error. Then, a robust adaptive control method for underactuated ship course with the consideration of sideslip angle is studied by designing a sliding mode surface with integral term and combining with the reaching law, and the stability of the proposed controller system is proved by the Lyapunov stability theory.

1 Definition and Lemma

Definition 1: homogeneity. For a continuous scalar function $V(x)$: $\mathbf{R}^n \rightarrow \mathbf{R}$, V has homogeneity σ [15] with respect to $(r_1, ..., r_n)$ when the following condition is met: for arbitrary real number $\lambda > 0$, there are a number $\sigma > 0$ and a vector $(r_1, ..., r_n) \in \mathbf{R}^n > 0$, with $r_i > 0$ $(i = 1, 2, ..., n)$, to ensure that $V(\lambda^{r_1} x_1, \cdots, \lambda^{r_n} x_n)$ equals $\lambda^d V(x_1, \cdots, x_n)$. For a vector function $\boldsymbol{f}(x)$: $\mathbf{R}^n \rightarrow \mathbf{R}^n$, $\boldsymbol{f}$ has homogeneity d [16] with respect to $(r_1, ..., r_n) \in \mathbf{R}^n > 0$ when the following condition is satisfied: for an arbitrary $\lambda > 0$, there is $(r_1, ..., r_n) \in \mathbf{R}^n > 0$, with $r_i > 0$ $(i = 1, 2, ..., n)$ to make $\boldsymbol{f}(x)$ satisfied when $f_i(\lambda^{r_1} x_1, \cdots, \lambda^{r_n} x_n)$ equals $\lambda^{r_i + d} f_i(x_1, \cdots, x_n)$, with $i = 1, 2, ..., n$ and $d > -\min\{r_i, i = 1, 2, ..., n\}$.

Lemma 1: suppose that there is a continuously differentiable function $V(x) > 0$: $U_1 \rightarrow \mathbf{R}$, $U_1 \subseteq U \in \mathbf{R}^n$, then

$$\dot{V}(x,t) \leqslant -cV^{\alpha}(x,t), \quad \forall x \in U_1 \backslash \{0\} \tag{1}$$

where U stands for the entire state space; set U_1 is the domain of the independent variable x; V^α is the α-order power of V; t is time; constant $c > 0$ and $0 < \alpha < 1$ show that the system is locally stable within finite time. For an arbitrary initial condition $x(t_0) \in U_1$, the convergence time satisfies $T \leqslant V^{1-\alpha}(x(t_0), t_0)/c(1-\alpha)$ [17], and t_0 is the initial time.

Lemma 2: suppose that there is a continuously differentiable function $V(x) > 0$: $U_1 \rightarrow \mathbf{R}$, $U_1 \subseteq U \in \mathbf{R}^n$, then

$$\dot{V}(x,t) \leqslant -c_1 V^{\alpha}(x,t) + c_2 V(x,t), \quad \forall x \in U_1 \backslash \{0\} \tag{2}$$

where constants c_1 and $c_2 > 0$, and $0 < \alpha < 1$ show that the system is locally stable within finite time. For an arbitrarily initial condition $x(t_0) \in \{U_1 \cap U_2\}$, the convergence time satisfies $T \leqslant \ln(1-(c_2/c_1)V^{1-\alpha}(x_0, t_0))/(c_2\alpha - c_2)$, and $U_2 = \{x | V^{1-\alpha}(x, t) \leqslant c_1/c_2\}$ [18].

Lemma 3: for arbitrary $x_i \in \mathbf{R}$ $(i = 1, 2, ..., n)$ and real number $0 < p \leqslant 1$, the equation is [19]

$$\left(\sum_{i=1}^{n} |x_i|\right)^p \leqslant \sum_{i=1}^{n} |x_i|^p \leqslant n^{1-p} \left(\sum_{i=1}^{n} |x_i|\right)^p \tag{3}$$

Lemma 4: for arbitrary $x_i \in \mathbf{R}$ $(i = 1, 2, ..., n)$ and real number $p > 1$, the equation is [20]

$$\sum_{i=1}^{n} |x_i|^p \leqslant \left(\sum_{i=1}^{n} |x_i|\right)^p \leqslant n^{p-1} \left(\sum_{i=1}^{n} |x_i|\right)^p \tag{4}$$

2 Model building

Based on the six-degree of freedom (6-DoF) model of underactuated ships, a 3-DoF underactuated ship model in the surge, sway, and yaw directions is established without the coupling between the surge/sway/yaw and the heave/roll/pitch. It is assumed that the inertial matrix, the added mass matrix, and the damping matrix in the model are diagonal matrices, and the aforementioned assumption holds true when the ship possesses three planes of symmetry. The port and starboard of most ships are symmetrical; however, it is unnecessary to consider the up-down symmetry when a ship sails in a horizontal plane. The fore-aft asymmetry of ships means that the off-diagonal terms of the inertial and damping matrices are non-zero. However, compared with the main diagonal terms, these off-diagonal terms are extremely small. On the basis of the above settings, the mathematical model of surface ships can be simplified as [21]

$$\begin{cases} \dot{u} = \dfrac{m_{22}}{m_{11}}vr - \dfrac{d_u}{m_{11}}u - \displaystyle\sum_{i=2}^{3}\dfrac{d_{ui}}{m_{11}}|u|^{i-1}u + \dfrac{1}{m_{11}}\tau_u + \dfrac{1}{m_{11}}\tau_{wu}(t) \\ \dot{v} = -\dfrac{m_{11}}{m_{22}}ur - \dfrac{d_v}{m_{22}}v - \displaystyle\sum_{i=2}^{3}\dfrac{d_{vi}}{m_{22}}|v|^{i-1}v + \dfrac{1}{m_{22}}\tau_{wv}(t) \\ \dot{r} = \dfrac{(m_{11}-m_{22})}{m_{33}}uv - \dfrac{d_r}{m_{33}}r - \displaystyle\sum_{i=2}^{3}\dfrac{d_{ri}}{m_{11}}|r|^{i-1}r + \\ \qquad \dfrac{1}{m_{33}}\tau_r + \dfrac{1}{m_{33}}\tau_{wr}(t) \\ \dot{\psi} = r \end{cases} \tag{5}$$

where ψ is the actual course in a fixed coordinate system, (°); u and v are the surge and sway velocities of the ship, respectively, m/s; r is the yaw velocity, rad/s; $m_{jj}\,(1 \leqslant j \leqslant 3)$ is a positive constant, indicating the inertial coefficient of the ship with added mass; d_u, d_v, d_r, d_{ui}, d_{vi}, and d_{ri} stand for the hydrodynamic damping coefficients in the surge, sway, and yaw directions, respectively; the unknown time-varying terms $\tau_{wu}(t)$, $\tau_{wv}(t)$, and $\tau_{wr}(t)$ are the environmental disturbances caused by wind, waves and currents, respectively; τ_u stands for the propulsion of the surface ship, N, and is provided by propellers or water jets; τ_r is the yaw torque, N·m, and is produced by changing the speed of each propeller or water jet, which indicates that course can only be controlled when the surge speed is non-zero. Therefore, an independent control system is designed to control the surge speed in this paper.

When the rudder is in the middle of the position, a ship that sails straight along the direction of the longitudinal section will not be subjected to a lateral force due to the symmetry of water flow. When the rudder has an angular deflection, it will be subjected to a lateral force due to the changed symmetry of water flow, and the point of action of lateral force will generate a torque around the center of gravity of the ship. Under the action of the torque, the ship will deflect relative to the water flow, and a sideslip angle β between the longitudinal section and the direction of the flow velocity can be defined as follows.

$$\beta = \arctan\left(\frac{v}{u}\right) \tag{6}$$

In order to simplify the controller design, this paper will use ESO to estimate the total disturbance in the yaw direction of the model. Therefore, for the design of the course controller, the 3-DoF underactuated ship model in Eq. (5) is simplified as

$$\begin{cases} \dot{\psi} = r \\ \dot{r} = f_r(t) + \dfrac{1}{m_{33}}\tau_r - g_r(t) + \dfrac{1}{m_{33}}\tau_{wr}(t) \end{cases} \tag{7}$$

where $f_r(t) = \dfrac{m_{11}-m_{22}}{m_{33}}uv$, $g_r(t) = -\dfrac{d_r}{m_{33}}r - \displaystyle\sum_{i=2}^{3}\dfrac{d_{ri}}{m_{11}}|r|^{i-1}$.

Let

$$w_r = f_r(t) + \frac{1}{m_{33}}\tau_{wr}(t)$$

$$\boldsymbol{w} = \left[\frac{1}{m_{11}}\tau_{wu}, \frac{1}{m_{22}}\tau_{wv}, \frac{1}{m_{33}}\tau_{wr} + f_r(t)\right]^{\mathrm{T}}$$

Assumption 1: the external disturbance is bounded, namely $|\tau_{wu}(t)| \leqslant \tau_{wu\max} < \infty$, $|\tau_{wv}(t)| \leqslant \tau_{wv\max} < \infty$, $|\tau_{wr}(t)| \leqslant \tau_{wr\max} < \infty$.

Assumption 2: since the energy of the external disturbance is limited, it is reasonable to assume that the derivative of $\boldsymbol{w}$ is bounded, namely $\|\dot{\boldsymbol{w}}\| \leqslant \varDelta$, where $\varDelta$ is the upper bound of $\dot{\boldsymbol{w}}$.

3 Control system

3.1 Course prefiltering and sideslip angle compensation

In order to avoid a large change rate in the ship course, this paper adds a prefilter to the control system to smooth the desired course, thus ensuring the robustness of the sliding mode controller. The main function of the prefilter is to filter the originally desired course ψ_{r} and achieve a smooth transition of the reference course ψ_{d} and the course change rate $\dot{\psi}_{\mathrm{d}}$, thus avoiding the higher requirements for the control gain and improving the controller performance. The form of the second-order prefilter used in this paper is as follows:

$$\ddot{\psi}_{\mathrm{d}} + \lambda_1\dot{\psi}_{\mathrm{d}} + \lambda_2\psi_{\mathrm{d}} = \lambda_3\psi_{\mathrm{r}} \tag{8}$$

where λ_i (i = 1, 2, 3) stands for the undetermined prefilter parameters.

The time-varying sideslip angle caused by external disturbance is so small that its influence is usually ignored with zero value in the ship course control; however, the sideslip angle has a certain influence on the tracking error in practice. Therefore, the course control with sideslip angle correction is taken into account in this paper, as shown in Fig. 1. In the figure, ψ_{h} is the actual course; ψ_{d} is the reference course after the prefiltering, and $\psi_{\mathrm{h}}-\psi_{\mathrm{d}}$ stands for the initial course error. In the existence of a sideslip angle, there is a sideslip angle between the actual motion direction of the ship and the expected tangential direction [8], and then the expected course ψ_{da} and the course error e_{a} based on the sideslip angle correction are

$$\psi_{\mathrm{da}} = \psi_{\mathrm{d}} - \beta \tag{9}$$

$$e_{\mathrm{a}} = \psi_{\mathrm{h}} - \psi_{\mathrm{da}} \tag{10}$$

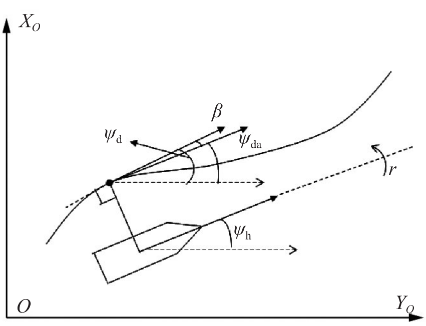

Fig. 1 The expected course with sideslip angle correction

3.2 Controller

3.2.1 Design of SMC law

In order to ensure the characteristics of automatic maintenance and tracking in the ship course, a closed-loop feedback control system is employed to study the tracking problem in the ship course. According to the principle of SMC, the sliding mode controller is designed with the idea of error feedback. In this paper, the designed sliding mode surface s with the integral term is as follows:

$$s = \dot{e} + b_1 e + b_2 \int_0^t |e|^p \mathrm{sgn}(e)\mathrm{d}\tau \tag{11}$$

where $0 < p < 1$ is a tunable parameter; b_1 and b_2 are tunable gain parameters; τ is the time integral variable; $e = e_{\mathrm{a}}$ stands for the corrected course error.

Buffeting will inevitably occur in SMC. This is mainly because the gain of the term of discontinuous sign function needs to be sufficiently large to guarantee robustness. In order to reduce the impact of sliding mode buffeting, a reaching law is used to improve the phenomenon. In this paper, the SMC based on the exponential reaching law is utilized to ensure that the moving points can reach the sliding mode within a limited time.

$$\dot{s} = \ddot{e} + b_1\dot{e} + b_2|e|^p\mathrm{sgn}(e) = -k_1 s - k_2\mathrm{sgn}(s) \tag{12}$$

The control law is solved as follows:

$$\tau_r = m_{33}\left(-f_r(t) + g_r(t) + \ddot{\psi}_r - b_1\dot{e} - b_2|e|^p\mathrm{sgn}(e) - \frac{1}{m_{33}}\tau_{wr}(t) - k_2\mathrm{sgn}(s) - k_1 s \right) \tag{13}$$

where k_1 and k_2 are positive constants.

In view of the Lyapunov function $V = \frac{1}{2}s^2$, its derivative can be taken, and the following equation is obtained.

$$\dot{V} = s\dot{s} = s(-k_1 s - k_2\mathrm{sgn}(s)) \leqslant -k_1 s^2 - k_2|s| \leqslant -\frac{k_1}{2}V \tag{14}$$

3.2.2 ESO design

To ensure tracking accuracy, FTESO is used to estimate and compensate for the total disturbance terms composed of the uncertainty and the external disturbance. The system structure is obtained by combining with the sliding mode controller, as shown in Fig. 2.

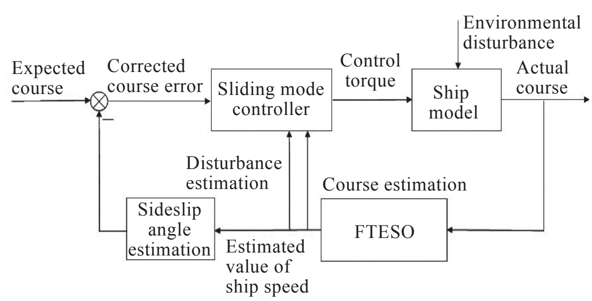

Fig. 2 Control system of the ship course

Here, $\boldsymbol{\eta}$ equals $[u, v, r]^{\mathrm{T}}$; $\hat{\boldsymbol{w}}$ is the state vector of the system expansion, which contains unknown external disturbance and internally unmodeled dynamic terms; the observer estimation error $z_1 = \boldsymbol{\eta} - \hat{\boldsymbol{\eta}}$; the extended state error $z_2 = \boldsymbol{w} - \hat{\boldsymbol{w}}$. Then, the FTESO in the following form is obtained:

$$\begin{cases} \dot{\hat{\boldsymbol{\eta}}} = \boldsymbol{f}(u,v,r) + \boldsymbol{\tau} + \boldsymbol{g}(u,v,r) + \\ \qquad \hat{\boldsymbol{w}} + m_1\mathrm{sig}^{\alpha_1}(z_1) + n_1\mathrm{sgn}(z_1) \\ \dot{\hat{\boldsymbol{w}}} = m_2\mathrm{sig}^{\alpha_2}(z_1) + n_2\mathrm{sgn}(z_1) \end{cases} \tag{15}$$

where

$$\boldsymbol{f}(u,v,r) = \begin{bmatrix} \dfrac{m_{22}}{m_{11}}vr \\ -\dfrac{m_{11}}{m_{22}}ur \\ 0 \end{bmatrix}$$

$$\boldsymbol{g}(u,v,r) = \begin{bmatrix} -\dfrac{d_u}{m_{11}}u - \displaystyle\sum_{i=2}^{3}\dfrac{d_{ui}}{m_{11}}|u|^{i-1} \\ -\dfrac{d_v}{m_{22}}v - \displaystyle\sum_{i=2}^{3}\dfrac{d_{vi}}{m_{22}}|v|^{i-1} \\ g_r(t) \end{bmatrix}$$

$$\mathrm{sig}^{\alpha}(z_1) = |z_1|^{\alpha}\mathrm{sgn}(z_1)$$

$$\boldsymbol{\tau}=\left[\frac{1}{m_{11}}\tau_u,\ 0,\ \frac{1}{m_{33}}\tau_r\right]^{\mathrm{T}}$$

and $\frac{1}{2}<\alpha_1<1, \alpha_2=2\alpha_1-1,\ m_i>0, n_i>0\,(i=1,2)$, are the observer design parameters.

The observer stability is proven as follows.

The equation of the observational error system of FTESO is

$$\begin{cases}\dot{\boldsymbol{z}}_1=\boldsymbol{z}_2-m_1\mathrm{sig}^{\alpha_1}(\boldsymbol{z}_1)-n_1\mathrm{sgn}(\boldsymbol{z}_1)\\ \dot{\boldsymbol{z}}_2=\dot{\boldsymbol{w}}-m_2\mathrm{sig}^{\alpha_2}(\boldsymbol{z}_1)-n_2\mathrm{sgn}(\boldsymbol{z}_1)\end{cases} \tag{16}$$

Let's put aside temporarily the two terms, $-n_1\mathrm{sgn}(\boldsymbol{z}_1)$ and $\dot{\boldsymbol{w}}-n_2\mathrm{sgn}(\boldsymbol{z}_1)$ in Eq. (16), the error system can be expressed as

$$\begin{cases}\dot{\boldsymbol{z}}_1=\boldsymbol{z}_2-m_1\mathrm{sig}^{\alpha_1}(\boldsymbol{z}_1)\\ \dot{\boldsymbol{z}}_2=-m_2\mathrm{sig}^{\alpha_2}(\boldsymbol{z}_1)\end{cases} \tag{17}$$

Let $\sigma=\alpha_1\alpha_2$. According to definition 1, it can be inferred that the system (Eq. (17)) has a homogeneity α_1-1 with respect to weights (1, α_1). The differentiable function can be defined as $V_\alpha=\boldsymbol{Z}^{\mathrm{T}}\boldsymbol{PZ}$, and $V_\alpha>0$, where $\boldsymbol{Z}=[\boldsymbol{Z}_1^T,\boldsymbol{Z}_2^{\mathrm{T}}]^{\mathrm{T}}=[[\mathrm{sig}^{\frac{1}{\sigma}}(\boldsymbol{z}_1)]^{\mathrm{T}}, [\mathrm{sig}^{\frac{1}{\sigma\alpha_1}}(\boldsymbol{z}_2)]^{\mathrm{T}}]^{\mathrm{T}}$, and $\boldsymbol{P}$ is the solution of the Lyapunov equation $\boldsymbol{A}^{\mathrm{T}}\boldsymbol{P}+\boldsymbol{PA}=-\boldsymbol{I}_6$, with $\boldsymbol{I}_i\,(i=2, 3, 4, ...)$ being the i-th-order identity matrix. The system matrix can be defined as

$$\boldsymbol{A}=\begin{bmatrix}-m_1\boldsymbol{I}_3 & \boldsymbol{I}_3\\ -m_2\boldsymbol{I}_3 & 0\end{bmatrix}$$

and $\boldsymbol{A}$ is the Hurwitz matrix. It is known from the Reference [15] that V_α is the Lyapunov function of the system (Eq. (17)), and $\boldsymbol{L}_{f\alpha}V_\alpha$ is the Lie derivative of V_α along the vector field $\boldsymbol{f}_\alpha$ by making $\boldsymbol{f}_\alpha$ be the vector field of the system (Eq. (17)). Therefore, it can be inferred that V_α and $\boldsymbol{L}_{f\alpha}V_\alpha$ have homogeneity $2/\sigma$ and $2/\sigma+(\alpha_1-1)$ with respect to weights (1, α_1), respectively. The following inequation can be obtained from the Literature [22]:

$$\boldsymbol{L}_{f_\alpha}V_\alpha\leqslant -c_1V_\alpha{}^{\varepsilon} \tag{18}$$

Where $c_1=-\max\limits_{\{\boldsymbol{Z}:\,V_\alpha=1\}}\boldsymbol{L}_{f_\alpha}V_\alpha(\boldsymbol{Z})$; $\varepsilon=1+\dfrac{\sigma\alpha_1}{2}-\dfrac{\sigma}{2}<1$.

The Lyapunov function of the error system (Eq. (16)) is designed as follows.

$$V_1=\boldsymbol{Z}^{\mathrm{T}}\boldsymbol{PZ} \tag{19}$$

The derivative of Eq. (19) is taken and

$$\dot{V}_1=\boldsymbol{L}_{f_\alpha}V_\alpha+2\boldsymbol{Z}^{\mathrm{T}}\boldsymbol{P}\cdot\begin{bmatrix}\dfrac{-\mathrm{diag}\left(|\boldsymbol{z}_1|^{\left(\frac{1}{\sigma}-1\right)}\right)n_1\mathrm{sgn}(\boldsymbol{z}_1)}{\sigma}\\ \dfrac{-\mathrm{diag}\left(|\boldsymbol{z}_2|^{\left(\frac{1}{\sigma\alpha_1}-1\right)}\right)[\dot{\boldsymbol{w}}-n_2\mathrm{sgn}(\boldsymbol{z}_1)]}{\sigma\alpha_1}\end{bmatrix} \tag{20}$$

By substituting Eq. (18) into Eq. (20), this paper obtains

$$\dot{V}_1\leqslant -c_1V_1{}^{\varepsilon}+\frac{2n_1\|\boldsymbol{Z}\|\lambda_{\max}(\boldsymbol{P})\left(\sum\limits_{m=1}^{3}|z_{1,m}|^{\left(\frac{1}{\sigma}-1\right)}\right)}{\sigma}+\frac{2(\varDelta+n_2)\|\boldsymbol{Z}\|\lambda_{\max}(\boldsymbol{P})\left(\sum\limits_{m=1}^{3}|z_{2,m}|^{\left(\frac{1}{\sigma\alpha_1}-1\right)}\right)}{\sigma\alpha_1} \tag{21}$$

where $\lambda_{\max}(\boldsymbol{P})$ is the largest eigenvalue of $\boldsymbol{P}$. According to Lemma 3 and the inequation $(a+b+c)^2\leqslant 3(a^2+b^2+c^2)$, the following inequation can be achieved:

$$\begin{aligned}&\left(\sum_{m=1}^{3}|z_{1,m}|^{\left(\frac{1}{\sigma}-1\right)}\right)\leqslant 3^{\sigma}\left(\sum_{m=1}^{3}|z_{1,m}|^{\frac{1}{\sigma}}\right)^{1-\sigma}\leqslant 3^{\frac{1+\sigma}{2}}\|\boldsymbol{z}_1\|^{1-\sigma}\\ &\left(\sum_{m=1}^{3}|z_{2,m}|^{\left(\frac{1}{\sigma\alpha_1}-1\right)}\right)\leqslant 3^{\sigma\alpha_1}\left(\sum_{m=1}^{3}|z_{2,m}|^{\frac{1}{\sigma\alpha_1}}\right)^{1-\sigma\alpha_1}\leqslant 3^{\frac{1+\sigma\alpha_1}{2}}\|\boldsymbol{z}_2\|^{1-\sigma\alpha_1}\end{aligned} \tag{22}$$

By substituting Eq. (22) into Eq. (21), the following equation is obtained:

$$\begin{aligned}\dot{V}_1&\leqslant -c_1V_1{}^{\varepsilon}+\frac{2\times 3^{\frac{1+\sigma}{2}}n_1\lambda_{\max}(\boldsymbol{P})\|\boldsymbol{Z}\|^{2-\sigma}}{\sigma}+\frac{2\times 3^{\frac{1+\sigma\alpha_1}{2}}(\varDelta+n_2)\lambda_{\max}(\boldsymbol{P})\|\boldsymbol{Z}\|^{2-\sigma\alpha_1}}{\sigma\alpha_1}\leqslant\\ &-c_1V_1{}^{\varepsilon}+c_2V_1{}^{1-\frac{\sigma}{2}}+c_3V_1{}^{1-\frac{\sigma\alpha_1}{2}}\end{aligned} \tag{23}$$

where

$$c_2=\frac{2\times 3^{\frac{1+\sigma}{2}}n_1\lambda_{\max}(\boldsymbol{P})}{\sigma\lambda_{\min}^{1-\frac{\sigma}{2}}(\boldsymbol{P})}$$

$$c_3=\frac{2\times 3^{\frac{1+\sigma\alpha_1}{2}}(\varDelta+n_2)\lambda_{\max}(\boldsymbol{P})}{\sigma\alpha_1\lambda_{\min}^{1-\frac{\sigma\alpha_1}{2}}(\boldsymbol{P})}$$

In consideration of $0<1-\dfrac{\sigma}{2}<1-\dfrac{\sigma\alpha_1}{2}<\varepsilon<1$, Eq. (23) will be further analyzed in two cases.

1) When $V_1\geqslant 1$, $\dot{V}_1\leqslant -c_1V_1{}^{\varepsilon}+c_4V_1$ and $c_4=c_2+c_3$; it can be inferred from lemma 2 that the time needed for V_1 to converge to $V_1=1$ can be expressed as $t_1\leqslant \ln[1-(c_4/c_1)V_1^{1-\varepsilon}(0)]/(c_4\varepsilon-c_4)$.

2) When $V_1<1$, $\dot{V}_1\leqslant -c_1V_1{}^{\varepsilon}+c_4V_1{}^{1-\frac{\sigma}{2}}$, and the parameter c_0 satisfies $0<c_0<1-\frac{c_4}{c_1}$, and then $\dot{V}_1\leqslant -c_1c_0V_1^{\varepsilon}-[c_1(1-c_0)\quad V_1^{\varepsilon-1+\frac{\sigma}{2}}-c_4]V_1^{1-\frac{\sigma}{2}}$. If $V_1{}^{\varepsilon-1+\frac{\varepsilon}{2}}>\dfrac{c_4}{c_1(1-c_0)}$ holds true, then $\dot{V}_1\leqslant -c_1c_0V_1{}^{\varepsilon}$, and V_1 is monotonically decreasing; if $V_1{}^{\varepsilon-1+\frac{\varepsilon}{2}}<\dfrac{c_4}{c_1(1-c_0)}$, in accordance with lemma 1, the following equation can be obtained $t_2\leqslant\dfrac{V_1{}^{1-\varepsilon}(t_1)}{c_1c_0(1-\varepsilon)}$.

Eventually, V_1 will converge to $V_1<\left(\dfrac{c_4}{c_1(1-c_0)}\right)^{\frac{2}{\sigma\alpha_1}}$ within a finite time $T=t_1+t_2$, and the estimation error can be expressed in the following form

$$\|\boldsymbol{Z}\|\leqslant\frac{1}{\sqrt{\lambda_{\min}(\boldsymbol{P})}}\left(\frac{c_4}{c_1(1-c_0)}\right)^{\frac{1}{\sigma\alpha_1}} \tag{24}$$

According to Lemma 3, there is

$$\|(z_1,z_2)\| \leqslant \sum_{m=1}^{3}(|z_{1,m}|^{\frac{1}{\sigma}})^{\sigma}+\sum_{m=1}^{3}(|z_{2,m}|^{\frac{1}{\sigma\alpha_1}})^{\sigma\alpha_1} \leqslant 3^{1-\sigma}\left(\sum_{m=1}^{3}(|z_{1,m}|^{\frac{1}{\sigma}})^{\sigma}\right)+3^{1-\sigma\alpha_1}\left(\sum_{m=1}^{3}(|z_{2,m}|^{\frac{1}{\sigma\alpha_1}})^{\sigma\alpha_1}\right) \leqslant 3^{1-\frac{\sigma}{2}}\|z_1\|^{\sigma}+3^{1-\frac{\sigma\alpha_1}{2}}\|z_2\|^{\sigma\alpha_1} \tag{25}$$

Finally, the estimation error of velocity and the ESO error can converge into the compact set Ω which is expressed as

$$\Omega=\left\{(z_1,z_2)|\|(z_1,z_2)\| \leqslant \frac{3^{1-\frac{\sigma}{2}}}{\sqrt{\lambda_{\min}(\boldsymbol{P})}^{\sigma}}\left(\frac{c_4}{c_1(1-c_0)}\right)^{\frac{1}{\alpha_1}}+\frac{3^{1-\frac{\sigma\alpha_1}{2}}}{\sqrt{\lambda_{\min}(\boldsymbol{P})}^{\sigma\alpha_1}}\left(\frac{c_4}{c_1(1-c_0)}\right)\right\} \tag{26}$$

3.3 Analysis of system stability

The design of the sliding mode controller based on FTESO is expressed as the following theorem.

Theorem 1: for the ship course control system (Eq. (17)), an ESO (Eq. (15)) is designed; the sliding mode surface is expressed by Eq. (11) by using the estimated sideslip angle $\hat{\beta}$ = arctan ($\hat{v}/\hat{u}$), and the sliding mode controller is designed as follows:

$$\tau_r=m_{33}(-\hat{w}_r+\hat{g}_r(t)+\ddot{\psi}_{\mathrm{da}}-b_1\hat{e}_{\mathrm{a}}-b_2|\hat{e}_{\mathrm{a}}|^p\mathrm{sgn}(\hat{e}_{\mathrm{a}})-k_1s-k_2\mathrm{sgn}(s)) \tag{27}$$

where $\hat{w}_r=\hat{f}_r(t)+\dfrac{1}{m_{33}}\hat{\tau}_{wr}$; $\psi_{\mathrm{da}}=\psi_{\mathrm{d}}-\hat{\beta}$; $\hat{e}_{\mathrm{a}}=\hat{\psi}-\psi_{\mathrm{da}}$; $\hat{\dot{e}}_{\mathrm{a}}=\hat{r}-\dot{\psi}_{\mathrm{da}}$. System tracking error asymptotically converges to zero.

Proof: the Lyapunov function is chosen as

$$V=\frac{1}{2}s^2 \tag{28}$$

Let $e_{\mathrm{b}}=|e_{\mathrm{a}}|^p\mathrm{sgn}(e_{\mathrm{a}})$ and take the derivative of v, and substitutes Eq. (27) into Eq. (28), then the following equation is obtained after rearrangement.

$$\begin{aligned}\dot{V}=s\dot{s}=s[\ddot{\psi}-\ddot{\psi}_{\mathrm{da}}+b_1(\dot{\psi}-\dot{\psi}_{\mathrm{da}})+b_2|e_{\mathrm{a}}|^p\mathrm{sgn}(e_{\mathrm{a}})]=\\ s[(w_r-\hat{w}_r)+(g_r(t)-\hat{g}_r(t))+b_1(r-\hat{r})+\\ b_2(e_{\mathrm{b}}-\hat{e}_{\mathrm{b}})-k_2\mathrm{sgn}(s)-k_1s]\leqslant -k_1s^2-k_2|s|+\\ |[(w_r-\hat{w}_r)+(g_r(t)-\hat{g}_r(t))+b_1(r-\hat{r})+b_2(e_{\mathrm{b}}-\hat{e}_{\mathrm{b}})]s|\end{aligned} \tag{29}$$

Since FTESO ensures that all estimation errors are sufficiently small, $k_2 \geqslant (w_r-\hat{w}_r)+(g_r(t)-\hat{g}_r(t))+b_1(r-\hat{r})+b_2(e_{\mathrm{b}}-\hat{e}_{\mathrm{b}})$ can be guaranteed as long as an appropriate k_2 is chosen; therefore,

$$\dot{V}\leqslant -k_1s^2=-2k_1V \tag{30}$$

For a better control effect, a steep saturation function is chosen and defined as

$$\mathrm{sat}(s)=\begin{cases}1, & s>\varepsilon_1\\ ks, & |s|\leqslant\varepsilon_1,\ k=\dfrac{1}{\varepsilon_1}\\ -1, & s<-\varepsilon_1\end{cases} \tag{31}$$

to approximate the sign function in the controller; ε_1 is the minimum value. In the limiting case where ε_1 tends to be zero, the saturation function is approximately the sign function, and the control law is taken as

$$\tau_r=m_{33}(-\hat{w}_r+\hat{g}_r(t)+\ddot{\psi}_{\mathrm{da}}-b_1\hat{e}_{\mathrm{a}}-b_2|\hat{e}_{\mathrm{a}}|^p\mathrm{sgn}(\hat{e}_{\mathrm{a}})-k_1s-k_2\mathrm{sat}(s)) \tag{32}$$

Therefore, the control system is asymptotically stable, and $\lim\limits_{t\to\infty}s=0$; then, it is known from Eq. (11) that the course tracking error e_{a} converges to zero asymptotically. The proof is complete.

4 Analysis of simulation results

In order to verify the effectiveness of the proposed controller, the entire course system was considered. In this paper, the modeling tool Simulink in Matlab was employed to build the entire system model, and simulation applications were carried out. The relevant parameters in the model (Eq. (5)) can be found in the Literature [22], i.e., m_{11} = 120 × 10^3, m_{22} = 177.9 × 10^3, m_{33} = 636 × 10^5; d_u = 215 × 10^2, d_v = 147 × 10^3, d_r = 802 × 10^4, d_{u2} = 0.2d_u, d_{u3} = 0.1d_u; d_{v2} = 0.2d_v, d_{v3}=0.1d_v; d_{r2} = 0.2d_r , d_{r3} = 0.1d_r. In this paper, the parameters selected for the design are shown in Table 1. Surge speed was controlled by an independent control system, and the PID controller designed based on ESO in this paper was used to make the ship surge at a speed of 7 m/s; in addition, the input constraint for yaw control was τ_m = 7 × 10^8 N·m. The initial velocity was set to 6 m/s, and the expected course angles were 20°, −20°, and 0°, respectively; the simulation step size and simulation time were set to 0.01 s and 150 s, respectively. Suppose that the environmental disturbances in the simulation are τ_{wu} = 150 × $10^3$$dr$, τ_{wr} = 900 × $10^5$$dr$, and τ_{wv} = 2 × 10^3× (1 + 0.3cos(0.4t)), where dr is the tertiary wave model and is expressed as follows:

$$dr=y(s)=h(s)\omega(s) \tag{33}$$

where $y(s)$ stands for the expression of the tertiary wave model; $\omega(s)$ refers to the process of zero-mean Gaussian white noise with a power spectrum density of 0.1; $h(s)$ is the transfer function of a second-order wave, and

$$h(s)=K_\omega s\Big/(s^2+2\omega_0\zeta s+\omega_0{}^2) \tag{34}$$

where ζ is the damping factor; ω_0 is the wave frequency, ω_0 = 4.85/T_ω, and T_ω is the wave period; K_ω = 2$\zeta\omega_0\sigma_\omega$, and $\sigma_\omega=\sqrt{0.018\,5T_\omega h_{1/3}}$ with $h_{1/3}$ being the significant wave height. The specific parameters are given as follows: T_ω = 4 s, $h_{1/3}$ = 0.8 m, ζ = 0.1, K_ω = 0.053, σ_ω = 0.218, ω_0 = 1.21, and ε_1 = 0.2.

Table 1 The parameters under different control methods

Control method	Controller					Observer				
	k_1	k_2	p	b_1	b_2	m_1	m_2	n_1	n_2	α_1
With sideslip angle	20	3	0.6	4.8	0.1	10	300	0.01	0.01	0.75
Without sideslip angle	10	2	0.6	5	0.3	15	350	0.01	0.01	0.75

To ensure the reliability of simulation results, this paper makes a simulation comparison between the linear ESO-based backstepping method and the FTESO-based SMC method proposed in this paper, and the simulation results are shown in Fig. 3−Fig. 7. Identical initial conditions and relevant parameters in different simulation models are kept consistent. In the figures, "SMC+FTESO−sideslip angle correction" is the SMC method considering sideslip angle correction; "SMC+FTESO−non-sideslip angle correction" is the SMC method without considering sideslip angle correction, and "backstepping+LESO" stands for the backstepping method combining with linear ESO.

It can be seen from Fig. 3(a) that the ship with the consideration of sideslip angle correction can reach the expected course faster (the expected value is reached within 4 s after the course change). However, for the method without considering sideslip angle correction and the conventional backstepping method, they take 8 s or even longer to reach a stable state. Fig. 3(b) shows the yaw torque of the controller without considering input saturation. It can be seen from the figure that the torque is far beyond the limit of the normal use of the rudder when the ship's course changes. In order to solve this problem, this paper adds input constraints when designing the course controller with sideslip angle correction.

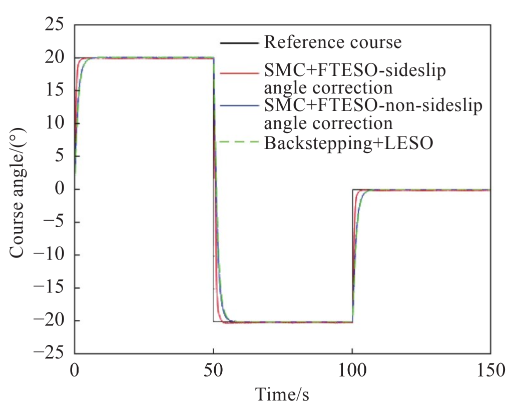

(a) Actual course

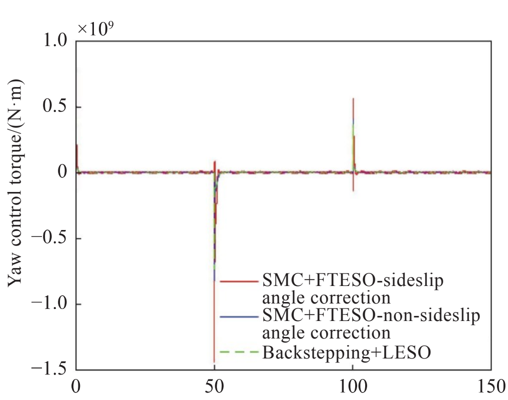

(b) Yaw control torque

Fig. 3 Comparison of heading angles and yaw torque of the controllers without input constraint

Fig. 4 shows the comparison of the courses and errors of three different controllers after input saturation (with constraints). It can be seen from the figure that after the control input is constrained, the courses and errors remain unchanged.

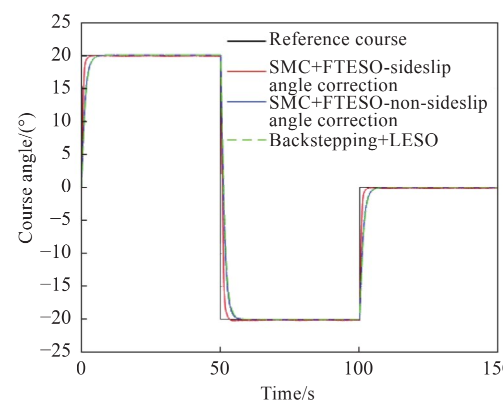

(a) Actual course

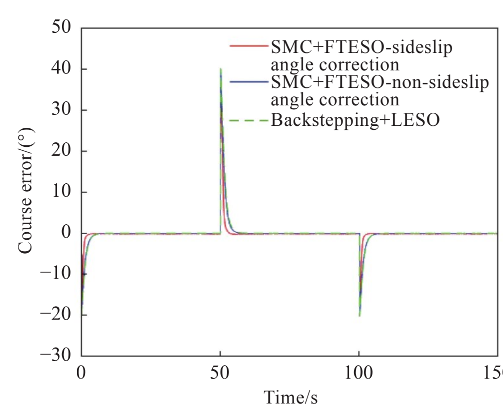

(b) Course error

Fig. 4 Comparison of course angles and errors of the controllers with input constraint

Fig. 5 shows the sideslip angle values estimated by the observer. It can be seen from the figure that the sideslip angle has always existed in the course of ship sailing, and it will change abruptly when the course changes, although its value is small. Therefore, the ship course with the sideslip angle correction can improve the performance of the course control and reduce the course error.

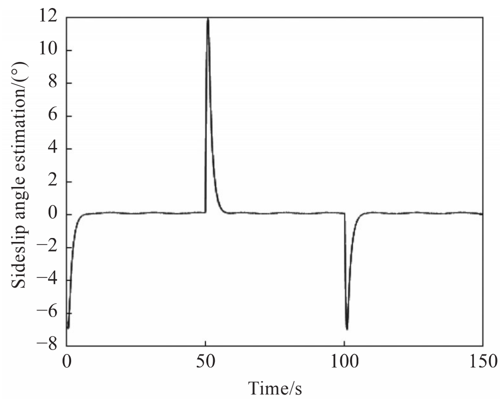

Fig. 5 Estimated value of sideslip angle

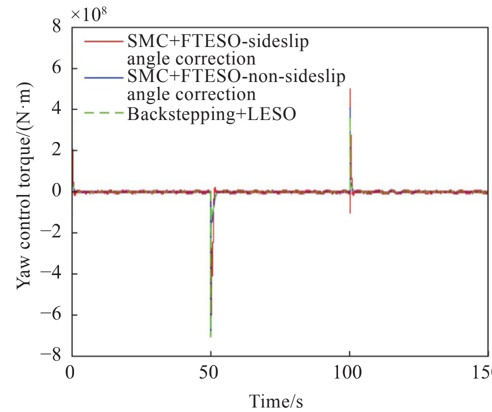

Fig. 6 Comparison of yaw torque of the controllers with input constraint

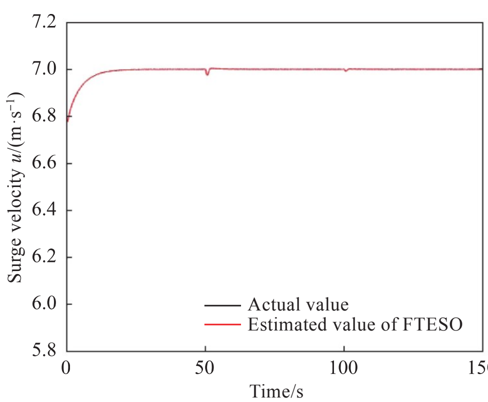

(a) Estimated value of surge velocity

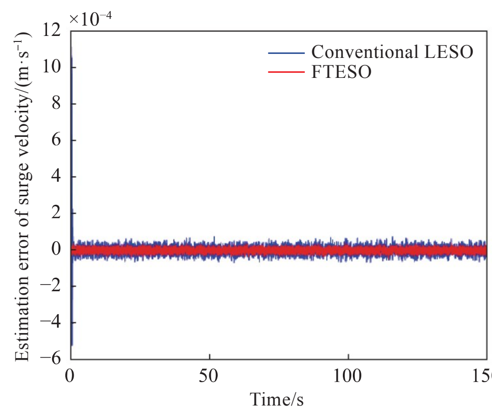

(b) Comparison of estimation error of surge

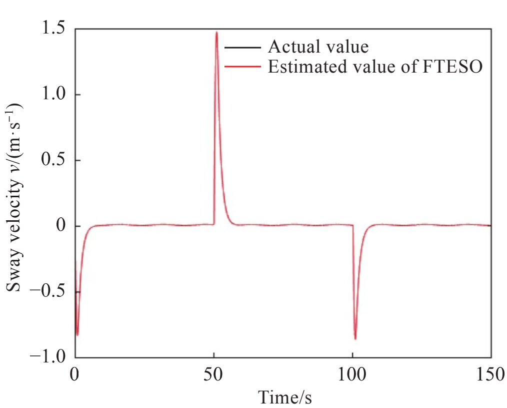

(c) Estimated value of sway velocity

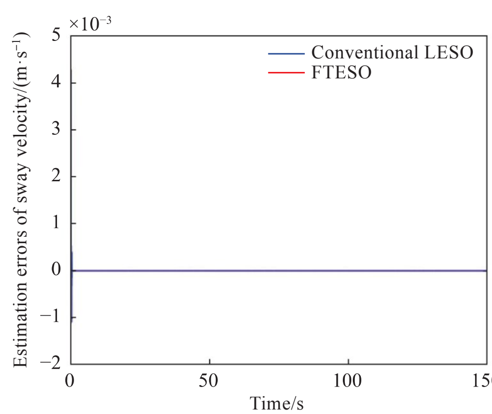

(d) Comparison of estimation errors of sway velocity

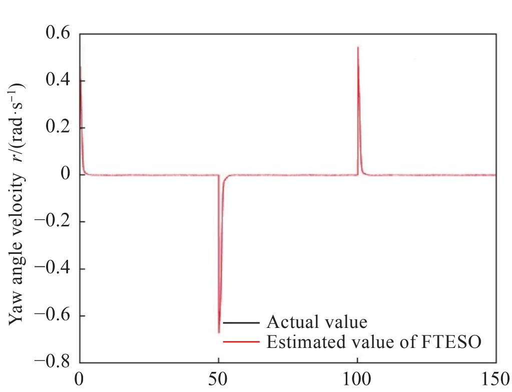

(e) Estimated value of yaw angle velocity

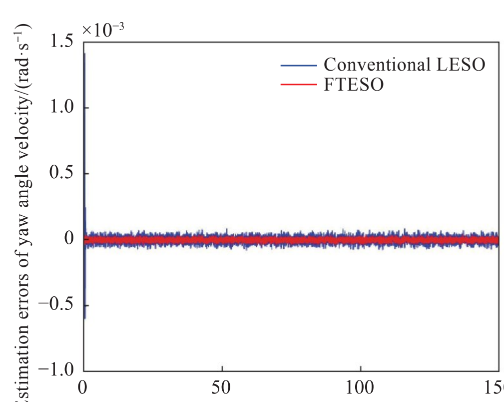

(f) Comparison of estimation errors of yaw angle velocity

Fig. 7 The estimated values and errors of velocity in the surge, sway, and yaw directions with input constraint

The yaw torque with input constraint is shown in Fig. 6. It can be seen from the figure that the yaw torque has been reduced accordingly.

According to the final course tracking effect, the SMC method designed in this paper gives itself no significant advantages compared with the conventional linear ESO-based backstepping method; however, the analysis from the perspective of the observer shows that the FTESO designed in this paper has better observational performance. Fig. 7 shows the estimated velocities and errors of the two observers in the surge, sway, and yaw directions. The estimated error of the yaw velocity with the FTESO maintains within $\pm 4\times10^{-5}$ rad/s, while the conventional LESO has a maximum error of 1.4×10^{-3} rad/s in the initial time and becomes stable within $\pm 6\times10^{-5}$ rad/s after an adjustment of 0.98 s. The estimation performance of the observer for the surge velocity u and sway velocity v is also important due to the sideslip angle correction. The estimation error of the FTESO for the surge velocity always maintains within $\pm 4\times10^{-5}$ m/s while the traditional LESO has a maximum error of 1.12×10^{-3} m/s in the initial time and a convergence time of 0.99 s, and the error stably fluctuates within $\pm 6\times10^{-5}$ m/s. Although the observational error of LESO in estimating the sway velocity v can eventually stay around $\pm 2\times10^{-7}$ m/s, its convergence time of 1.15 s is still longer than that of FTESO, i. e. 0.06 s; moreover, the error at the initial moment reaches 4.3×10^{-3} m/s, while the maximum estimation error of FTESO is only 6.68×10^{-5} m/s.

5 Conclusions

In this paper, the sideslip angle correction is considered in the design of the course tracking controller with the 3-DoF motion model of the underactuated ship on the water surface as the object; unlike the direct calculation of sideslip angle by using relative speed, FTESO is used for real-time estimation of the sideslip angle, thereby greatly improving the ship's course tracking performance. The simulation results show that the observational performance of FTESO is excellent compared with that of the conventional linear observer. The estimation of the total disturbance term is compensated in the design of the reaching law-based sliding model controller, which weakens the buffeting effect and guarantees a strong anti-interference capability of the course control system when the course tracking error converges to zero. Moreover, the saturation function is used to constrain the yaw torque in the paper, which is of excellent practical significance. Although certain constraints are imposed on the input torque in the paper, there is still room for improvement, and the following study will continue to study the input saturation and enhance the control accuracy by improving the algorithm.

References

[1] WU R, DU J L, SUN Y Q, et al. Ship course tracking control based on the state feedback linearization and ESO [J]. Journal of Dalian Maritime University, 2019, 45 (3): 93−99 (in Chinese).

[2] ZHANG X K, ZHANG Q, REN H X, et al. Linear reduction of backstepping algorithm based on nonlinear decoration for ship course-keeping control system [J]. Ocean Engineering, 2018, 147: 1−8.

[3] PERERA L P, SOARES C G. Pre-filtered sliding mode control for nonlinear ship steering associated with disturbances [J]. Ocean Engineering, 2012, 51: 49−62.

[4] SHEN Z P, ZOU T Y. Adaptive dynamic surface course control for an unmanned sailboat with unknown control direction [J]. Journal of Harbin Engineering University, 2019, 40 (1): 94−101 (in Chinese).

[5] ZHU D J, MA N, GU X C. Adaptive fuzzy compensation control for nonlinear ship course-keeping [J]. Journal of Shanghai Jiao Tong University, 2015, 49 (2): 250−254, 261 (in Chinese).

[6] WANG D W, FU Y. Model predict control method based on higher-order observer and disturbance compensation control [J]. Acta Automatica Sinica, 2020, 46 (6): 1220−1228 (in Chinese).

[7] PERERA L P, SOARES C G. Lyapunov and Hurwitz based controls for input-output linearisation applied to nonlinear vessel steering [J]. Ocean Engineering, 2013, 66: 58−68.

[8] HU C, WANG R R, YAN F J, et al. Robust composite nonlinear feedback path-following control for underactuated surface vessels with desired-heading amendment [J]. IEEE Transactions on Industrial Electronics, 2016, 63 (10): 6386−6394.

[9] BEVLY D A, RYU J, GERDES J C. Integrating INS sensors with GPS measurements for continuous estimation of vehicle sideslip, roll, and tire cornering stiffness [J]. IEEE Transactions on Intelligent Transportation Systems, 2006, 7 (4): 483−493.

[10] WANG N, SUN Z, YIN J C, et al. Finite-time observer based guidance and control of underactuated surface vehicles with unknown sideslip angles and disturbances [J]. IEEE Access, 2018, 6: 14059−14070.

[11] LI Y, BAI X E, XIAO Y J. Ship course sliding mode control system based on a novel extended state disturbance observer [J]. Journal of Shanghai Jiao Tong University, 2014, 48 (12): 1708−1713, 1720 (in Chinese).

[12] XIONG S F, WANG W H, LIU X D, et al. A novel extended state observer [J]. ISA Transactions, 2015, 58:

309−317.

[13] LIANG K, LIN X G, CHEN Y, et al. Adaptive sliding mode output feedback control for dynamic positioning ships with input saturation [J]. Ocean Engineering, 2020, 206: 107245.

[14] AN L, LI Y, CAO J, et al. Proximate time optimal for the heading control of underactuated autonomous underwater vehicle with input nonlinearities [J]. Applied Ocean Research, 2020, 95: 102002.

[15] PERRUQUETTI W, FLOQUET T, MOULAY E. Finite time observers: application to secure communication [J]. IEEE Transactions on Automatic Control, 2008, 53 (1): 356−360.

[16] ROSIER L. Homogeneous Lyapunov function for homogeneous continuous vector field [J]. Systems and Control Letters, 1992, 19 (6): 467−473.

[17] HONG Y G, WANG J K, CHENG D Z. Adaptive finite-time control of nonlinear systems with parametric uncertainty [J]. IEEE Transactions on Automatic Control, 2006, 51 (5): 858−862.

[18] SHEN Y J, XIA X H. Semi-global finite-time observers for nonlinear systems [J]. Automatica, 2008, 44 (12): 3152−3156.

[19] HARDY G H, LITTLEWOOD J E, PÓLYA G. Inequalities [M]. Cambridge: Cambridge University Press, 1952.

[20] ZOU A M, DE RUITER A H J, KUMAR K D. Distributed finite-time velocity-free attitude coordination control for spacecraft formations [J]. Automatica, 2016, 67: 46−53.

[21] DO K D, JIANG Z P, PAN J. Robust adaptive path following of underactuated ships [J]. Automatica, 2004, 40 (6): 929−944.

[22] BHAT S P, BERNSTEIN D S. Geometric homogeneity with applications to finite-time stability [J]. Mathematics of Control, Signals, and Systems, 2005, 17 (2): 101−127.

基于FTESO和漂角补偿的船舶航向滑模控制

储瑞婷，刘志全*

上海海事大学 航运技术与控制工程交通运输行业重点实验室，上海 201306

摘　要：［**目的**］为提高水面欠驱动船舶的航向跟踪性能，减小航向误差，研究一种基于有限时间扩张状态观测器(FTESO)的船舶航向滑模控制方法。［**方法**］首先，采用预滤波器减小船舶转向时较大的航向变化率影响，利用扩张状态观测器对时变漂角进行估计，然后通过估计出的漂角及时修正航向误差。为简化控制器设计，艏摇方向上的外部扰动和内部不确定项由观测器同时估计，并在控制器设计中进行补偿。选取含积分项的滑模面，结合FTESO设计滑模控制律，并考虑输入饱和约束，最终通过李雅普诺夫理论证明控制系统的稳定性。［**结果**］仿真结果显示，所研究的控制方法使水面船舶能够在较短的时间内减小航向跟踪误差并收敛至0。［**结论**］研究成果可为水面船舶航向跟踪控制设计提供参考。

关键词：航向控制；漂角；滑模控制；有限时间扩张状态观测器；输入饱和约束